*Communication*

# ESI-MS/MS Identification of a Bradykinin-Potentiating Peptide from Amazon *Bothrops atrox* Snake Venom Using a Hybrid Qq-*oa*TOF Mass Spectrometer

**Antonio Coutinho-Neto** [1]**, Cleópatra A. S. Caldeira** [1]**, Gustavo H. M. F. Souza** [2]**,**
**Kayena D. Zaqueo** [1]**, Anderson M. Kayano** [1]**, Rodrigo S. Silva** [1]**, Juliana P. Zuliani** [1,3]**,**
**Andreimar M. Soares** [1]**, Rodrigo G. Stábeli** [1,3] **and Leonardo A. Calderon** [1,3,]*****

[1] Center of Biomolecules Study Applied to Health, Fiocruz Rondônia, Oswaldo Cruz Foundation, Porto Velho, RO 76820-245, Brazil; E-Mails: antonio.dnabrasil@gmail.com (A.C.-N.); cleobiol@gmail.com (C.A.S.C.); kayena@gmail.com (K.D.Z.); kayano@unir.br (A.M.K.); simoesdg@gmail.com (R.S.S.); zuliani.juliana@gmail.com (J.P.Z.); andreimarsoares@gmail.com (A.M.S.); stabeli@fiocruz.br (R.G.S.)

[2] MS Applications Development Laboratory, Waters Corporation, Alphaville, SP 06455-020, Brazil; E-Mail: gustavo_souza@waters.com

[3] Medicine Department, Federal University of Rondônia, Porto Velho, RO 76801-059, Brazil

***** Author to whom correspondence should be addressed; E-Mail: calderon@fiocruz.br; Tel.: +55-6921822118; Fax: +55-6932196000.

**Abstract:** A bradykinin-potentiating peptide (BPP) from Amazon *Bothrops atrox* venom with *m/z* 1384.7386 was identified and characterized by collision induced dissociation (CID) using an ESI-MS/MS spectra obtained in positive ion mode on a hybrid Qq-*oa*TOF mass spectrometer, Xevo G2 QTof MS (Waters, Manchester, UK). *De novo* peptide sequence analysis of the CID fragmentation spectra showed the amino acid sequence ZKWPRPGPEIPP, with a pyroglutamic acid and theoretical monoisotopic *m/z* 1384.7378, which is similar to experimental data, showing a mass accuracy of 0.6 ppm. The peptide is homologous to other BPP from *Bothrops moojeni* and was named as BPP-BAX12.

**Keywords:** bioactive peptide; BPP; pyroglutamic acid; pyrrolidonecarboxylic acid; *de novo* peptide sequencing

## 1. Introduction

Snake venoms have been recognized as an extensible source of bioactive peptides with potential biotechnological applications in medicine [1]. Due to their high degree of target specificity, venom toxins have been increasingly used as lead compounds in the development of drug prototypes [2]. One of the most successful examples has been Captopril®, an antihypertensive drug based on a bradykinin-potentiating peptide (BPP) isolated from Brazilian *Bothropoides* (*Bothrops*) *jararaca* venom [3,4]. The BPP family comprises a class of angiotensin-I converting enzyme (ACE) inhibitors with different lengths (5 to 14 amino acid residues) found in venoms produced by snakes, scorpions, spiders and amphibians [5]. Generally, BPPs have a conserved *N*-terminal pyroglutamate residue (Z) and two consecutive proline residues at the *C*-terminal region [6,7]. This work describes the identification and characterization of a new BPP from Amazon *Bothrops atrox* snake venom.

## 2. Materials and Methods

### 2.1. Venom

*Bothrops atrox* specimens collected around the city of Porto Velho, State of Rondônia, Brazil were kept at Fiocruz Rondônia bioterium in order to be used for venom production under authorization emitted by IBAMA (licence number 27131-1) and CGEN (licence number 010627/2011-1). The crude venom was dehydrated and stored at a temperature of −20 °C in the Amazon Venom Bank at CEBio.

### 2.2. Peptide Isolation

The purification of BPP-BAX12 was performed using 50 mg of crude venom, which was divided fractioned into two fractions on a size exclusion chromatography column using a Superdex peptide-10/300GL column (GE Healthcare) equilibrated with 50 mmol/L Tris-HCl buffer (pH 7.4) and carried out at a flow rate of 0.5 mL/min. The second fraction produced, which was related to peptides, was re-chromatographed under the same conditions resulting in eight fractions. The fourth fraction (37–43 min) was then lyophilized and stored for MS/MS analysis.

### 2.3. MS Parameters and Data Acquisition

ESI-MS spectra were obtained in positive ion mode on a hybrid Qq-*oa*TOF mass spectrometer—Xevo G2 QTof MS (Waters, Manchester, UK). Typical ESI-MS conditions were done in positive mode as follow: source temperature 80 °C, capillary voltage 2.8 kV, and cone voltage 35 V, resolution mode with an analogic-to-digital converter (ADC) mode, detector at 2825 V previously adjusted with leukine enkephalin (Leu-Enk) solution at 2 ng/μL. The instrument was automatically calibrated with sodium iodide solution through IntelliStart, integral part of MassLynx 4.1v acquisition software (Waters, Manchester, UK). Samples were re-suspended in a vial with a solution containing equal parts of water and methanol with 0.1% of formic acid for each sample to proceed ESI(+)-MS analysis. These solutions were then injected at a flow rate of 500 nL/min, using the fluid system installed in the Xevo G2 QTof MS panel controlled by the IntelliStart software and MS tune page. All MS spectra were acquired over the *m/z* 50–2000. MS/MS acquisition was performed using the

quadrupole with high discrimination for each *m/z* of interest. The collision energy was applied to the selected precursor ion and a collision-induced dissociation (CID) at the T-Wave collision cell filled with argon gas was used. 25 eV was applied to the collision cell depending on the precursor ion dissociation characteristics.

*2.4. MS/MS Analysis*

The MS/MS spectra were de-convoluted using MaxEnt 3 software (Waters, Manchester, UK) and then transferred to a PepSeq application into BioLynx software package and a Microsoft Excel file with data up to 120 counts in order to proceed with manual evaluation. The identification of the most common diagnostic peptide fragment ions (a$^+$, b$^+$, y$^+$-type) currently observed in low energy collisions and immonium ions for *de novo* peptide sequencing were performed manually using the program Microsoft Excel with data of monoisotopic mass of common and less common amino acid residues, terminal groups and post-translational modifications for the use in mass spectrometry calculated using the following atomic masses of the most abundant isotope of the elements: C = 12.0000000, H = 1.0078250, N = 14.0030740, O = 15.9949146, F = 18.9984033, P = 30.9737634, S = 31.9720718, Cl = 34.9688527, Br = 78.9183361. Fragments with intensity higher than 200 counts and mass accuracy between 0 and ± 17 ppm, according to the equation 1, was used for *de novo* peptide sequencing.

Mass accuracy (ppm) = 1,000,000 × (theoretical mass − measured mass)/theoretical mass

MassSeq application and *de novo* sequencing analysis and interpretation tool of the BioLynx software package was used in order to confirm manual analysis using the following peptide sequencing parameters: *m/z* tolerance of 0.03 for peptide and fragments and intensity threshold of 0.003%.

**3. Results and Discussion**

The mass spectrometric analysis of the fourth chromatographic fraction reveals a high intensity doubly protonated ion peak at *m/z* 692.8732 [M + 2H]$^{2+}$. The ion was selected and submitted to collision-induced dissociation (CID) with argon gas resulting in a mass spectrum (Figure 1), which was submitted to the identification of a$^+$, b$^+$, and y$^+$-type diagnostic fragments and immonium ions for *de novo* peptide sequence (Tables 1 and 2) [8]. The analysis revealed a 12 residue proline-rich peptide (Pyr-Lys-Trp-Pro-Arg-Pro-Gly-Pro-Glu-Ile/Leu-Pro-Pro) with a conserved consecutive two proline residues at the *C*-terminal region, a characteristic of the BPP family of ACE inhibitors [6,7], and a *N*-terminal pyroglutamic acid (Pyr), which could be derived from glutamine or glutamic acid residues, as observed in other currently described snake venom BPPs from Bothrops species. The measured peptide monoisotopic mass (1384.7386) and theoretical (1384.7378) was very similar, showing a mass accuracy of 0.6 ppm, which was also observed for the identified diagnostic fragment ions (Tables 1 and 2), thus showing the high precision of the analysis. Sequence similarity showed that the peptide is homologous to other BPP described for *B. moojeni* venom [6] and similar to others from *Bothrops neuwiedi* [1,9], *B. leucurus*, *B. erythromelas*, *B. alternatus* [10], *B. insularis* [1,10,11], *B. jararaca* [12,13], *B. jararacussu* [1,10,14], *B. cotiara* [13], and *B. fonsecai* [13] (Table 3). This peptide was named as Bradykinin-potentiating peptide BAX12.

**Figure 1**. Collision-induced dissociation spectra of BPP-BAX12. The deduced sequence is shown at the top of the MS/MS profile. The inset shows the assigned peptide sequence.
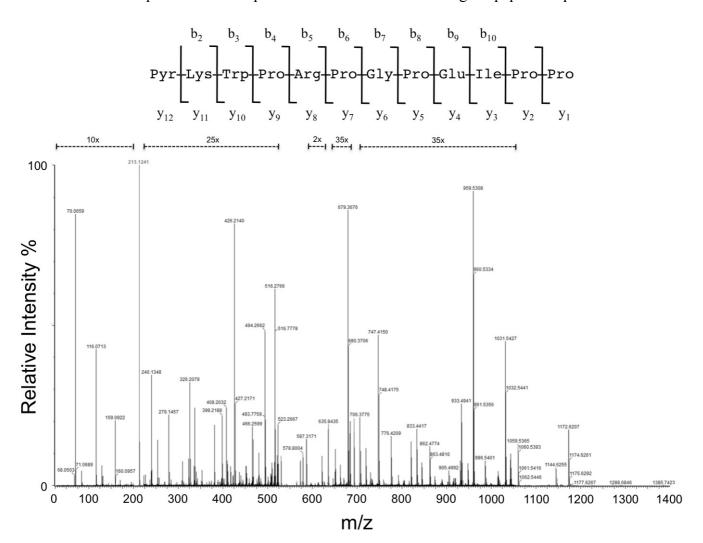
**Table 1.** Diagnostic peptide fragments (b, a and y-type ions) obtained by collision-induced dissociation with argon gas used for *de novo* peptide sequencing of BPP-BAX12.

| Aminoacid Residue | Fragment | Theoretical (m/z) | Measured (m/z) | Intensity (counts) | Accuracy (ppm) | Fragment | Theoretical (m/z) | Measured (m/z) | Intensity (counts) | Accuracy (ppm) | Fragment | Theoretical (m/z) | Measured (m/z) | Intensity (counts) | Accuracy (ppm) |
|---|---|---|---|---|---|---|---|---|---|---|---|---|---|---|---|
| Z | $b_1$ | 112.0399 | - | - | - | $a_1$ | 84.0688 | - | - | - | $y_{12}$ | 1384.7377 | 1384.7548 | $1.6 \times 10^2$ | 11.7 |
| K | $b_2$ * | 223.1083 | 223.1082 | $2.7 \times 10^3$ | 0.2 | $a_2$ * | 195.1134 | 195.1134 | $4.0 \times 10^3$ | −0.2 | $y_{11}$ | 1273.7057 | 1273.6853 | $1.6 \times 10^2$ | 16.0 |
|  | $b_2$ | 240.1348 | 240.1348 | $5.2 \times 10^4$ | 0.1 | $a_2$ | 212.1399 | 212.1405 | $6.1 \times 10^3$ | −2.9 | $y_{11}$ * | 1256.6792 | - | - | - |
| W | $b_3$ | 426.2141 | 426.2140 | $1.2 \times 10^5$ | 0.3 | $a_3$ | 398.2192 | 398.2188 | $3.3 \times 10^4$ | 1.0 | $y_{10}$ | 1145.6107 | 1145.6276 | $2.0 \times 10^5$ | 14.8 |
| P | $b_4$ | 523.2669 | 523.2667 | $2.9 \times 10^4$ | 0.4 | $a_4$ | 495.2720 | 495.2684 | $3.1 \times 10^4$ | 7.2 | $y_9$ | 959.5314 | 959.5308 | $9.9 \times 10^4$ | 0.6 |
| R | $b_5$ * | 662.3415 | 622.3417 | $7.0 \times 10^3$ | −0.4 | $a_5$ * | 634.3466 | 634.3317 | $3.7 \times 10^4$ | 23.4 | $y_8$ | 862.4786 | 862.4774 | $1.3 \times 10^4$ | 1.4 |
|  | $b_5$ | 679.3680 | 679.3676 | $9.3 \times 10^4$ | 0.6 | $a_5$ | 651.3731 | 651.3705 | $1.2 \times 10^4$ | 4.0 | $y_8$ * | 845.4520 | 845.4680 | $6.0 \times 10^3$ | −18.9 |
| P | $b_6$ | 776.4208 | 776.4209 | $1.7 \times 10^4$ | −0.2 | $a_6$ | 748.4259 | 748.4175 | $3.0 \times 10^4$ | 11.2 | $y_7$ | 706.3775 | 706.3775 | $2.3 \times 10^4$ | 0.0 |
| G | $b_7$ | 833.4422 | 833.4417 | $1.9 \times 10^4$ | −0.6 | $a_7$ | 805.4473 | 805.4473 | $1.8 \times 10^3$ | 0.0 | $y_6$ | 609.3248 | 609.3238 | $3.6 \times 10^2$ | 1.6 |
| P | $b_8$ | 930.4950 | 930.4941 | $8.4 \times 10^3$ | 1.0 | $a_8$ | 902.5001 | 902.5016 | $1.2 \times 10^3$ | −1.7 | $y_5$ | 552.3033 | 552.3032 | $4.8 \times 10^3$ | 0.2 |
| E | $b_9$ # | 1041.5273 | 1041.5265 | $2.0 \times 10^3$ | 0.8 | $a_9$ # | 1013.5321 | 1013.5197 | $4.4 \times 10^2$ | 12.2 | $y_4$ | 455.2505 | 455.2492 | $3.7 \times 10^2$ | 2.8 |
|  | $b_9$ | 1059.5376 | 1059.5365 | $5.0 \times 10^5$ | 1.0 | $a_9$ | 1031.5427 | 1031.5427 | $4.9 \times 10^4$ | 0.0 | $y_4$ # | 437.2399 | 437.2360 | $6.3 \times 10^3$ | 9.0 |
| I/L | $b_{10}$ | 1172.6206 | 1172.6207 | $6.6 \times 10^5$ | −0.1 | $a_{10}$ | 1144.6257 | 1144.6255 | $2.1 \times 10^5$ | 0.2 | $y_3$ | 326.2081 | 326.2079 | $4.9 \times 10^4$ | 0.7 |
| P | $b_{11}$ | 1269.6734 | - | - | - | $a_{11}$ | 1241.6785 | - | - | - | $y_2$ | 213.1241 | 213.1241 | $3.8 \times 10^6$ | −0.1 |
| P | $b_{12}$ | 1366.7261 | - | - | - | $a_{12}$ | 1338.7312 | - | - | - | $y_1$ | 116.0712 | 116.0713 | $1.6 \times 10^5$ | −1.2 |

Immonium ions detected Theoretical *m/z*, measured *m/z* (accuracy in ppm): Z 84.04496, 84.0446 [4.3]; K($-NH_3$) 84.08129, 84.08144 [−1.3]; R($-NH_3$) 112.08746, 112.0877 [−2.2]; W 159.09220, 159.0922 [0.0]; P 70.06568, 70.0659 [3.1]; I/L 86.09698, 86.0970 [−0.2]. * Loss of a neutral ammonia ($NH_3$) molecule from K or R side chains. # loss of a neutral $H_2O$ molecule from E side chain.

**Table 2.** Diagnostic internal fragments (b and a-type ions) ions obtained by collision-induced dissociation with argon gas used for *de novo* peptide sequencing of BPP-BAX12.

| Fragments | b-Type ions | | | | a-Type ions | | | |
|---|---|---|---|---|---|---|---|---|
| | Theoretical (*m/z*) | Measured (*m/z*) | Intensity (counts) | Accuracy (ppm) | Theoretical (*m/z*) | Measured (*m/z*) | Intensity (counts) | Accuracy (ppm) |
| KWPRPGP | 819.4629 | - | - | - | 791.46799 | - | - | - |
| KWPRPGP * | 802.4364 | 802.4401 | $2.3 \times 10^2$ | −4.6 | 774.44149 | - | - | - |
| KWPRPG | 722.4102 | - | - | - | 694.41529 | - | - | - |
| KWPRPG * | 705.3836 | 705.3939 | $8.2 \times 10^2$ | −14.6 | 677.38869 | 677.3793 | $1.0 \times 10^3$ | 13.9 |
| KWPRP | 665.3887 | - | - | - | 637.39379 | - | - | - |
| KWPRP * | 648.3622 | - | - | - | 620.36729 | - | - | - |
| KWPR | 568.3359 | - | - | - | 540.34099 | 540.3436 | $1.7 \times 10^2$ | −4.8 |
| KWPR * | 551.3094 | - | - | - | 523.31449 | - | - | - |
| KWP | 412.2349 | 412.2426 | $4.9 \times 10^2$ | −18.7 | 384.23999 | - | - | - |
| KWP * | 395.2083 | - | - | - | 367.21339 | - | - | - |
| KW | 315.1821 | 315.1797 | $2.2 \times 10^2$ | 7.6 | 287.18719 | - | - | - |
| KW * | 298.1556 | 298.1567 | $6.3 \times 10^2$ | −3.7 | 270.16069 | 270.1608 | $1.9 \times 10^3$ | −0.4 |
| WPRPGPEIP | 1030.5474 | 1030.5469 | $1.0 \times 10^3$ | 0.5 | 1002.5525 | 1002.5590 | $1.3 \times 10^2$ | −6.5 |
| WPRPGPEIP * | 1013.5209 | 1013.5197 | $4.4 \times 10^2$ | 1.1 | 985.5259 | - | - | - |
| WPRPGPEI | 933.4946 | 933.4941 | $2.8 \times 10^4$ | 0.5 | 905.4997 | 905.4992 | $5.0 \times 10^3$ | 0.5 |
| WPRPGPEI * | 916.4681 | 916.4681 | $2.5 \times 10^3$ | 0.0 | 888.4731 | 888.4796 | $9.8 \times 10^2$ | −7.3 |
| WPRPGPE | 820.4106 | 820.4102 | $1.5 \times 10^4$ | 0.5 | 792.4157 | 792.4160 | $3.4 \times 10^3$ | −0.4 |
| WPRPGPE * | 803.3841 | 803.3862 | $1.5 \times 10^3$ | −2.7 | 775.3891 | 775.3857 | $6.3 \times 10^2$ | 4.4 |
| WPRPGP | 691.3680 | 691.3715 | $7.7 \times 10^2$ | −5.1 | 663.3731 | - | - | - |
| WPRPGP * | 674.3415 | - | - | - | 646.3465 | 646.3524 | $3.0 \times 10^2$ | −9.1 |
| WPRPG | 594.3152 | 594.3206 | $2.4 \times 10^3$ | −9.1 | 566.3203 | - | - | - |
| WPRPG * | 577.2887 | 577.2831 | $1.9 \times 10^2$ | 9.6 | 549.2937 | - | - | - |
| WPRP | 537.2938 | - | - | - | 509.2989 | - | - | - |
| WPRP * | 520.2673 | - | - | - | 492.2723 | 492.2757 | $1.6 \times 10^2$ | −6.8 |
| WPR | 440.2410 | 440.2399 | $4.6 \times 10^3$ | 2.5 | 412.2461 | - | - | - |
| WPR * | 423.2145 | 423.2138 | $2.2 \times 10^3$ | 1.5 | 395.2195 | 395.2174 | $8.6 \times 10^2$ | 5.4 |
| WP | 284.1399 | - | - | - | 256.1450 | 256.1468 | $5.5 \times 10^2$ | −7.1 |
| PRPGPEIP | 844.4681 | 844.4672 | $7.8 \times 10^3$ | 1.1 | 816.4732 | - | - | - |
| PRPGPEIP * | 827.4416 | 827.4381 | $1.6 \times 10^2$ | 4.2 | 799.4466 | - | - | - |
| PRPGPEI/ RPGPEIP | 747.4153 | 747.4150 | $5.1 \times 10^4$ | 0.4 | 719.4204 | 719.4196 | $1.3 \times 10^4$ | 1.1 |
| PRPGPEI */RPGPEIP * | 730.3888 | 730.3976 | $4.4 \times 10^3$ | −12.1 | 702.3938 | 702.4028 | $1.4 \times 10^3$ | −12.7 |
| PRPGPE | 634.3313 | 634.3317 | $3.7 \times 10^4$ | −0.6 | 606.3364 | 606.3362 | $1.1 \times 10^4$ | 0.3 |
| PRPGPE * | 617.3048 | 617.3059 | $3.4 \times 10^3$ | −1.9 | 589.3098 | 589.3193 | $2.2 \times 10^3$ | −16.0 |
| PRPGP | 505.2887 | 505.2886 | $1.6 \times 10^3$ | 0.2 | 477.2938 | 477.295 | $3.9 \times 10^2$ | −2.5 |
| PRPGP * | 488.2622 | 488.2668 | $1.4 \times 10^2$ | −9.5 | 460.2672 | - | - | - |
| PRPG/RPGP | 408.2359 | 408.2354 | $2.2 \times 10^3$ | 1.2 | 380.2410 | 380.2346 | $5.6 \times 10^2$ | 16.8 |

**Table 2.** *Cont.*

| Fragments | b-Type ions | | | | a-Type ions | | | |
|---|---|---|---|---|---|---|---|---|
| | Theoretical (*m/z*) | Measured (*m/z*) | Intensity (counts) | Accuracy (ppm) | Theoretical (*m/z*) | Measured (*m/z*) | Intensity (counts) | Accuracy (ppm) |
| PRPG */RPGP * | 391.2094 | - | - | - | 363.2144 | - | - | - |
| PRP | 351.2145 | 351.2112 | $2.1 \times 10^3$ | 9.4 | 323.2196 | - | - | - |
| PRP * | 334.1880 | 334.1869 | $6.7 \times 10^2$ | 3.2 | 306.1930 | - | - | - |
| PR/RP | 254.1617 | 254.1616 | $2.2 \times 10^4$ | 0.4 | 226.1668 | - | - | - |
| PR/RP * | 237.1352 | 237.136 | $2.8 \times 10^3$ | −3.6 | 209.1402 | 209.1388 | $4.1 \times 10^2$ | 6.9 |
| RPGPEI | 650.3626 | 650.3616 | $4.7 \times 10^3$ | 1.5 | 622.3677 | - | - | - |
| RPGPEI * | 633.3361 | - | - | - | 605.3411 | 605.3397 | $1.2 \times 10^3$ | 2.4 |
| RPGPE | 537.2785 | 537.2814 | $2.9 \times 10^3$ | −5.4 | 509.2836 | 509.2862 | $2.2 \times 10^3$ | −5.1 |
| RPGPE * | 520.2520 | 520.2515 | $9.3 \times 10^2$ | 0.9 | 492.2570 | 492.2552 | $6.2 \times 10^2$ | 3.7 |
| RPG | 311.1832 | - | - | - | 283.1883 | - | - | - |
| RPG * | 294.1567 | 294.1559 | $2.4 \times 10^2$ | 2.6 | 266.1617 | - | - | - |
| IP | 211.1446 | 211.1445 | $3.1 \times 10^3$ | 0.5 | 183.14969 | 183.1503 | $1.2 \times 10^3$ | −3.3 |

**\*** Loss of a neutral ammonia ($NH_3$) molecule from K or R side chains.

**Table 3.** Sequence alignment between BPP-BAX12 and Pyroglutamate peptides/Bradykinin-potentiating (BPPs) sequences from others Bothrops species.

| BPP name | Sequence | Bothrops specie | Reference |
|---|---|---|---|
| BPP-BAX12 | ZKWPRPGPEIPP | *Bothrops atrox* | this work |
| - | ZKWPRPGPEIPP | *B. moojeni* | [6] |
| - | ZNWPRPGPEIPP | *B. moojeni* | [6] |
| BPP3_BOTNU, BPP13_BOTMO, BPP13_BOTLC, BPP13_BOTER, BPP13_BOTAL, BNP_BOTIN, BNP2_BOTJA, BNP1_BOTJA, Q8QG90_BOTIN, BNP_BOTJR [#] | ZGGWPRPGPEIPP | *B. neuwiedi, B. moojeni, B. leucurus, B. erythromelas, B. alternatus, B. insularis, B. jararaca, B. jararaca, B. insularis, B. jararacussu* | [1,9–13] |
| BPP-13a | ZGGWPRPGPEIPP | *B. cotiara, B. fonsecai* | [14] |
| BPP-13b | ZGGLPRPGPEIPP | *B. cotiara, B. fonsecai* | [14] |

[#] Entry name from UniProtKB.

## 4. Conclusions

Recent papers on venomics [15], proteome [16] and transcriptome [17] of *B. atrox* snake have shown an absence of BPP structures. However, only a single cluster that matched a 5' untranslated region of a BPP mRNA from *B. jararacussu* snake was found [11]. The BAX12 is the first peptide belonging to the BPP family of ACE inhibitor described for *Bothrops atrox*. The complete homology between BPP-BAX12 from *Bothrops moojeni* [6] and others BPPs could provide interesting information regarding the evolutionary relationship between Bothrops snake species.

**Acknowledgements**

**References**

1. Wermelinger, L.S.; Dutra, D.L.; Oliveira-Carvalho, A.L.; Soares, M.R.; Bloch, C., Jr.; Zingali, R.B. Fast analysis of low molecular mass compounds present in snake venom: Identification of ten new pyroglutamate-containing peptides. *Rapid Commun. Mass Spectrom.* **2005**, *19*, 1703–1708.

2. Fernandez, J.H.; Neshich, G.; Camargo, A.C.M. Using bradykinin-potentiating peptide structures to develop new antihypertensive drugs. *Genet. Mol. Res.* **2004**, *3*, 554–563.

3. Ferreira, S.H. A Bradykinin-potentiating factor (BPF) present in the venom of *Bothrops jararaca*. *Brit. J. Pharmacol.* **1965**, *24*, 163–169.

4. Smith, C.G.; Vane, J.R. The Discovery of Captopril. *FASEB J.* **2003**, *17*, 788–789.

5. Escoubas, P.; Quinton, L.; Nicholson, G.M. Venomics: Unravelling the complexity of animal venoms with mass spectrometry. *J. Mass Spectrom.* **2008**, *43*, 279–295.

6. Menin, L.; Perchuc, A.; Favreau, P.; Perret, F.; Michalet, S.; Schöni, R.; Wilmer, M.; Stöcklin, R. High throughput screening of bradykinin-potentiating peptides in *Bothrops moojeni* snake venom using precursor ion mass spectrometry. *Toxicon* **2008**, *51*, 1288–1302.

7. Ianzer, D.; Konno, K.; Marques-Porto, R.; Portaro, F.C.V.; Stöcklin, R.; Camargo, A.C.M.; Pimenta, D.C. Identification of five new bradykinin potentiating peptides (BPPs) from *Bothrops jararaca* crude venom by using electrospray ionization tandem mass spectrometry after a two-step liquid chromatography. *Peptides* **2004**, *25*, 1085–1092.

8. Seidler, J.; Zinn, N.; Boehm, M.E.; Lehmann, W.D. *De novo* sequencing of peptides by MS/MS. *Proteomics* **2010**, *10*, 634–649.

9. Ferreira, L.A.F.; Galle, A.; Raida, M.; Schrader, M.; Lebrun, I.; Habermehl, G. Isolation: Analysis and properties of three bradykinin-potentiating peptides (BPP-II, BPP-III, and BPP-V) from *Bothrops neuwiedi* venom. *J. Protein Chem.* **1998**, *17*, 285–289.

10. Souza, G.H.M.F.; Catharino, R.R.; Ifa, D.R.; Eberlin, M.N.; Hyslop, S. Peptide fingerprinting of snake venoms by direct infusion nano-electrospray ionization mass spectrometry: Potential use in venom identification and taxonomy. *J. Mass Spectrom.* **2008**, *43*, 594–599.

11. Cintra, A.C.O.; Vieira, C.A.; Giglio, J.R. Primary structure and biological activity of bradykinin potentiating peptides from Bothrops insularis snake venom. *J. Protein Chem.* **1990**, *9*, 221–227.

12. Hayashi, M.A.F.; Murbach, A.F.; Ianzer, D.; Portaro, F.C.V.; Prezoto, B.C.; Fernandes, B.L.; Silveira, P.F.; Silva, C.A.; Pires, R.S.; Britto, L.R.G.; *et al*. The C-type natriuretic peptide precursor of snake brain contains highly specific inhibitors of the angiotensin-converting enzyme. *J. Neurochem.* **2003**, *85*, 969–977.

13. Tashima, A.K.; Zelanis, A.; Kitano, E.S.; Ianzer, D.; Melo, R.L.; Rioli, V.; Sant'anna, S.S.; Schenberg, A.C.; Camargo, A.C.; Serrano, S.M. Peptidomics of three bothrops snake venoms: Insights into the molecular diversification of proteomes and peptidomes. *Mol. Cell. Proteomics* **2012**, *11*, 1245–1262.

14. Rioli, V.; Prezoto, B.C.; Konno, K.; Melo, R.L.; Klitzke, C.F.; Ferro, E.S.; Ferreira-Lopes, M.; Camargo, A.C.M.; Portaro, F.C.V. A novel bradykinin potentiating peptide isolated from *Bothrops jararacussu* venom using catallytically inactive oligopeptidase EP24.15. *FEBS J.* **2008**, *275*, 2442–2454.

15. Calvete, J.J.; Sanz. L.; Pérez, A.; Borges, A.; Vargas, A.M.; Lomonted, B.; Angulo, Y.; Gutiérrez, J.M.; Chalkidis, H.M.; Mourão, R.H.V.; *et al*. Snake population venomics and antivenomics of *Bothrops atrox*: Paedomorphism along its transamazonian dispersal and implications of geographic venom variability on snakebite management. *J. Proteomics* **2011**, *74*, 510–527.

16. Guércio, R.A.P.; Shevchenko, A.; Shevchenko. A.; López-Lozano, J.L.; Paba, J.; Sousa, M.V.; Ricart, C.A.O. Ontogenetic variations in the venom proteome of the Amazonian snake *Bothrops atrox*. *Proteome Sci*. **2006**, *4*, 14.

17. Neiva, M.; Arraes, F.B.M.; Souza, J.V.; Radis-Baptista, G.; Silva, A.R.B.P.; Walter, M.E.M.T.; Brigido, M.M.; Yamane, T.; Lopez-Lozano, J.L.; Astolfi-Filho, S. Transcriptome analysis of the Amazonian viper *Bothrops atrox* venom gland using expressed sequence tags (ESTs). *Toxicon* **2009**, *53*, 427–436.